RF-MEMS switching LC-tank network for multiband VCO

R. Gaddi*, A. Gnudi*, M. Bellei*, B. Margesin** and F. Giacomozzi**

* ARCES, University of Bologna
Viale Risorgimento 2, 40136 Bologna, Italy, rgaddi@arces.unibo.it
** ITC-irst, Povo (TN), Italy, margesin@itc.it

ABSTRACT

An LC-tank network with reconfigurable resonance frequency is designed and implemented fully in RF-MEMS technology. An ohmic switch with interdigitated signal-actuation electrodes is exploited in a shunt configuration for selectively bypassing an inductor. The resulting two alternative resonance frequencies are predicted by circuit simulations and validated through s-parameter based on-wafer characterisation. Frequencies of 1.375 GHz and 3.605 GHz are obtained for the up and down switch states, with Q-factors of 7.2 and 14.4 respectively. Lumped element equivalent circuit analysis identifies main loss mechanisms in lossy coupling to ground and ohmic contact series resistance.

Keywords: rf-mems switch, reconfigurable networks, rf oscillator, multi-band, vco

1 INTRODUCTION

In the search for reconfigurable multi-band and multi-standard wireless transceiver solutions, offering best performances in terms of power consumption, miniaturisation and frequency coverage, the exploitation of emerging MEMS technologies is increasingly raising the interest of the research community. Among different alternative approaches, recent efforts have focused on achieving low-loss reconfigurable passive networks based on MEMS switches. The aim is typically the implementation of multi-band impedance matching of low-noise or power amplifiers or tank circuits for voltage controlled oscillators (VCO) [1], [2]. Following this rationale, the present paper stems from a recently developed RF-MEMS technology based on high resistivity Silicon substrate and suspended gold membrane [3]. We propose the design of a switching dual frequency LC-tank, based on interdigitated ohmic switch [4], to be eventually combined with CMOS electronics for the implementation of a dual band RF oscillator. Measurement results on a fabricated prototype test structure are presented and provide for validation data for the simulation based design methodology.

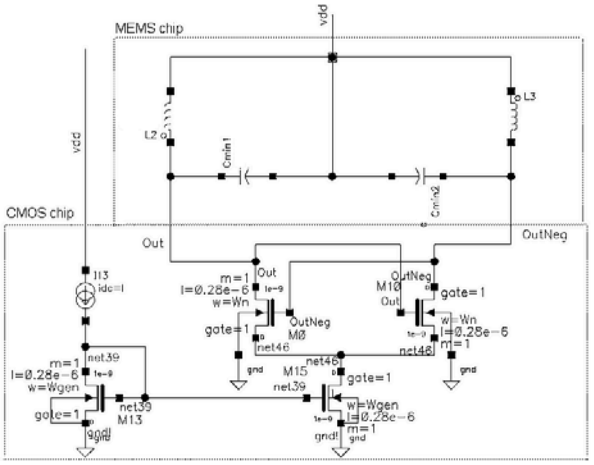

Figure 1: Schematic view of the simulated VCO in Cadence, made of CMOS electronics and the MEMS LC-tank.

2 LC-TANK DESIGN

Figure 1 shows a principle schematic of the adopted oscillator topology, identifying the MEMS technology based symmetric LC-tank. A typical differential construction was chosen, based on a pair of cross-coupled n-MOS transistors. In the preliminary design stage, the LC-tank was simply modelled as ideal components, while STM 0.13μm CMOS technology was used for the active part. The LC-tank network provides for both frequency selection and bias feed, and preliminary components' values are obtained through design tuning. Frequency band switching is allowed by having two alternative values for the inductance, which are to be implemented through two suspended spiral inductors in series and one RF-MEMS ohmic shunt switch in between. The actuation of the shunt switch creates an ohmic contact shorting out one of the two inductors and shifting the resonance frequency to the upper band. The resonators capacitance is implemented with a fixed metal-insulator-metal (MIM) capacitor in the same RF-MEMS technology.

Figure 2 shows a detailed schematic of half of the symmetric network, as implemented in Agilent EESOF ADS. Introducing empirical models of the inductors and the

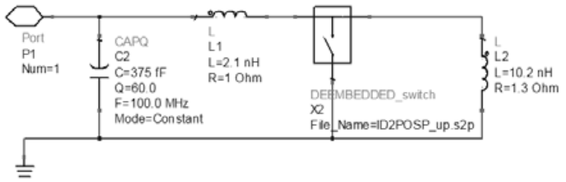

Figure 2: ADS simulation schematic of the ohmic shunt switch based LC-tank network.

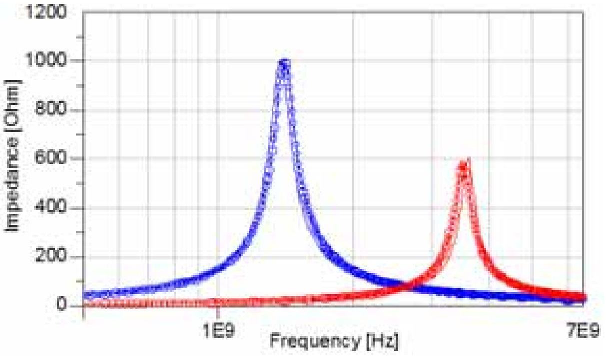

Figure 3: Measured data (lines) compared to ADS simulations (circles) for the LC-tank network of Fig. 2, after the correction of the input capacitance value by a 2.5 factor.

switch, extracted from previous on-wafer s-parameter measurement data, a second design stage leads to the optimisation of the capacitance and inductors values. During circuit simulation the switch is included in the analysis as a sub-circuit, which can be either defined through direct data look-up of previously measured s-parameters, or as a lumped element network extracted from RF measurements as described in [4]. In both cases, either the actuated or unactuated switch model can be placed in the simulation to investigate both frequency bands. Concerning the inductors, their available values and parasitic series resistances have been extracted from s-parameters measurements of single devices RF test structures. Values of inductors and capacitance were chosen at this stage to cover the GSM 1.8 GHz and the WLAN 5.5 GHz bands with the two MEMS switch states.

3 EXPERIMENTAL CHARACTERISATION AND DISCUSSION

Figure 4 shows the fabricated test structure of half of the symmetric LC network for on-wafer RF-characterisation. Measurements where performed through GSG RF probing, after 1-port SOL calibration on a separate Impedance Standard Substrate (ISS) from Cascade. Measured impedance magnitude data are shown in Fig. 3, giving the two resonance frequencies of 1.375 GHz and 3.605 GHz for the up-state and down-state respectively. The observed frequency mismatch compared to the original design can be attributed to two main factors. First, post-fabrication process characterisation identified issues with both the dielectric constant value (about 25% higher than the nominal 3.95) and thickness (reduced to 60nm from the nominal 100nm) for the low-temperature oxide (LTO) used for the MIM capacitor. Furthermore, no account was taken at design level of electromagnetic coupling between adjacent layout components. A simple increase of the value of the input capacitance by a factor of 2.5 gives the simulated results shown again in Fig. 3, that compare very well with the measured data. Nonetheless, only a correction by a factor of 2 is justified by the MIM capacitance technology issues, therefore further investigations are made through a post-layout electromagnetic simulation. The method of moments simulator of EESOF ADS, Momentum, is utilised. Figure 5 shows current density distributions on conductors obtained from simulations with the switch either in up-state and down-state configurations. Due to limitations of the 2.5D simulator, the down-state switch is modelled by placing fictituous connecting vias underneath the suspended plate, therefore creating a lossless connection to the underlying substrate metal. All simulations are also performed adopting lossless metalisations for obtaining a numerically manageable problem size. Despite of these several approximations, the EM simulation results approached quite well the measured resonance frequency values, giving 1.35±0.05 GHz and 3.4±0.1 GHz (frequency steps were also limited by total simulation time). This result could be obtained after allowing for the corrected post-fabrication values of oxide dielectric constant and thickness, therefore imputing the remaining frequency shift effect to the mainly capacitive coupling to adjacent ground metal layers, with current distribution effects that are clearly visible from Fig. 5.

The quality factor extracted from the measurement results is 7.2 and 14.4 for the up-state and down-state respectively. These values were somewhat lower than expected, and an analysis on the main loss mechanisms is performed through simulations based on the extracted equivalent lumped-element circuits for the switch, as reported in Fig. 6 [4]. Preliminary observations ruled out the inductors as being the primary source of losses, hence the focus is mainly on the switch. For each switch state, the lumped parameters were varied during simulation and an assessment is made of the resulting influence on the resonance quality factor.

In the up-state configuration, the most significant ef-

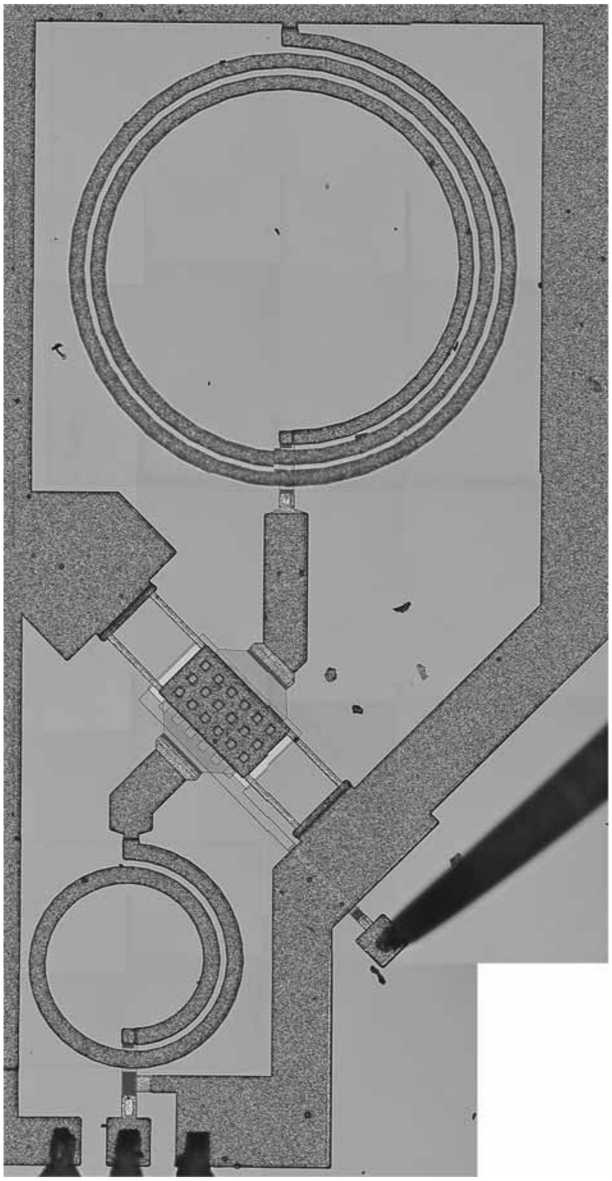

Figure 4: Optical image of the realised LC-tank based on an ohmic RF-MEMS shunt switch.

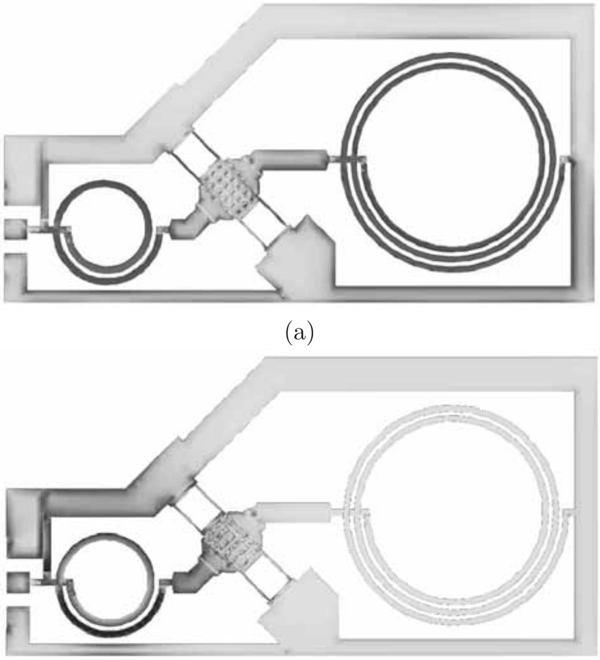

(a)

(b)

Figure 5: Electromagnetic simulation with ADS Momentum of the LC-tank with the switch either in (a) up-state (resonance at 1.35 GHz)) and (b) down-state (resonance at 3.4 GHz) configurations, showing current density on conductors.

fect results from ground coupling at both switch ports, namely related to the G_a and G_c conductances of Fig. 6. Figure 7 shows (left-side peaks) the expected x1.5 increase in quality factor attainable by halfing the values of these coupling terms.

On the other hand, the actuated switch has its dominant loss mechanism in the achievable value of ohmic contact resistance, named R_{switch} in Fig. 6. By assuming a reduction by half of this key parameter (extracted value is 1 Ω), again a x1.5 increase in the down-state quality factor is predicted from simulations, as shown in Fig. 7 (right-side peaks).

These identified key loss mechanisms can be tackled both at technology and design level. Lossy coupling effects are directly linked to the physical properties of the dielectrics, namely a TEOS oxide and a low-temperature oxide (LTO) layers [3]. The latter is also responsible for the MIM capacitance value increase discussed above, and further investigations on its final overall qualities are currently underway. Besides, alternative switch layouts that reduce coupling to ground, especially through the actuation electrodes, are being investigated.

On the other hand, the quality of the ohmic contact of the actuated switch can be improved by chosing different metallisations. The use of different metal coatings

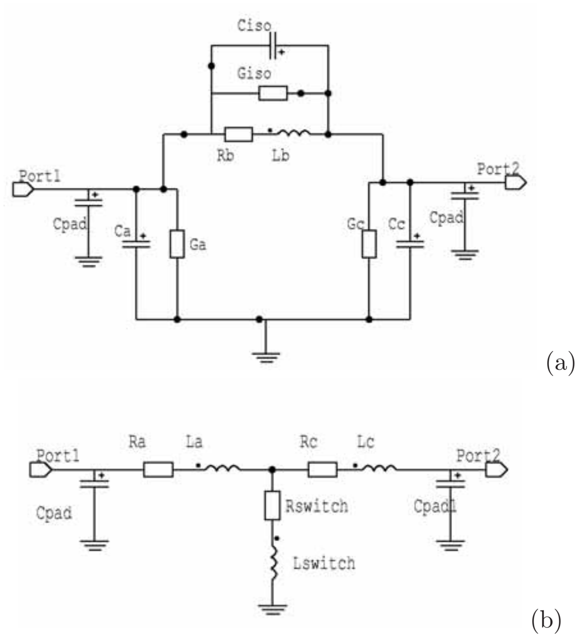

Figure 6: Lumped element equivalent circuits extracted from measured s-parameters for the single RF-MEMS ohmic shunt switch in its up-state (a) and down-state (b) configurations.

of the substrate electrode (made of Ti-TiN-Al-Ti-TiN multi-metal) is currently being examined. Furthermore, alternative layout design solutions aimed at optimizing contact force and total contact surface for minimal resistance still leave room for improvements, although the current interdigitated approach proved already to provide satisfying results.

4 CONCLUSION

An LC-tank network was designed fully in a developed RF-MEMS technology, aiming at covering two alternative frequency bands through network reconfigurability. An ohmic switch with interdigitated signal-actuation electrodes was utilised in shunt configuration, selectively shorting-out one inductor and allowing for two alternative resonance frequencies. Circuit simulations were validated by experimental results based on on-wafer characterisation of the LC-tank test structure. Frequencies of 1.375 and 3.605 GHz were obtained for the up and down switch states, with Q-factors of 7.2 and 14.4 respectively, resulting in a significant frequency shift from the original design (1.8 GHz - 5.5 GHz). Issues related to the LTO dielectric layer were identified as principal contributors to this incongruity. Furthermore, lumped element equivalent circuit analysis identified the main loss mechanisms in lossy couplings to ground and the series resistance of the ohmic contact.

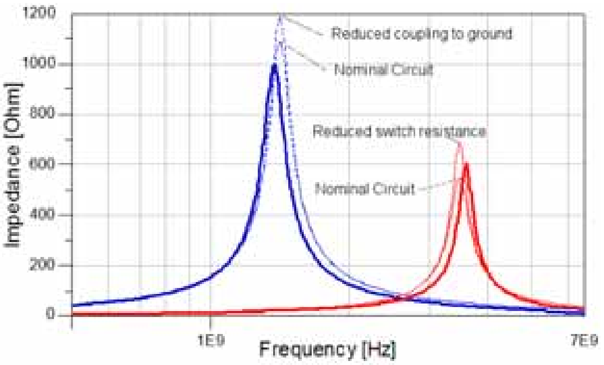

Figure 7: Measured data (thick lines) compared to ADS simulations (thin lines) for the LC-tank network adopting an extracted equivalent circuit for the MEMS switch. The effects of a reduction of substrate coupling and ohmic series resistance in the circuit are also shown.

5 ACKNOWLEDGEMENTS

This work was supported by the Italian Ministry for University and Research (MIUR) as part of the FIRB project "Enabling technologies for Wireless Reconfigurable Terminals" (RBNE01F582).

REFERENCES

[1] R.L. Borwick, et Al., "Variable MEMS Capacitors Implemented Into RF Filter Systems," IEEE Trans. MTT, Vol.51, pp.315-319, Jan 2003.

[2] J. Papapolymerou, et Al., "Reconfigurable Double-Stub Tuners Using MEMS Switches for Intelligent RF Front-Ends," IEEE Trans. MTT, Vol.51, pp.271-278, Jan 2003.

[3] F. Giacomozzi, M. Bellei, P. Farinelli, G. Mannocchi, R. Marcelli, B. Margesin, and V. Mulloni, "Electromechanical Aspects in the Optimization of the Transmission Characteristics of Series Ohmic RF-Switches," 5th Workshop on MEMS for MilliMeterwave Communications (MEMSWAVE2004), Uppsala University, Uppsala, Sveden, 30th June - 2nd July 2004, pp. C25-C28.

[4] R. Gaddi, M. Bellei, A. Gnudi, B. Margesin, F. Giacomozzi, "Interdigitated Low-Loss Ohmic RF-MEMS Switches," Proceedings of NSTI-Nanotech 2004, Boston, MA, USA, 7-11 March 2004, Vol. 2, pp.327-330.